


Article

Vegetation Productivity Dynamics in Response to Climate Change and Human Activities under Different Topography and Land Cover in Northeast China

Hui Li ^{1,2} , Hongyan Zhang ^{1,2,*}, Qixin Li ³, Jianjun Zhao ^{1,2} , Xiaoyi Guo ^{1,2} , Hong Ying ^{1,2},
Guorong Deng ^{1,2} , Wu Rihan ^{1,2} and Shuling Wang ⁴

¹ Key Laboratory of Geographical Processes and Ecological Security in Changbai Mountains, Ministry of Education, School of Geographical Sciences, Northeast Normal University, Changchun 130024, China; lih795@nenu.edu.cn (H.L.); zhaojj662@nenu.edu.cn (J.Z.); guoxy914@nenu.edu.cn (X.G.); hongy864@nenu.edu.cn (H.Y.); denggr272@nenu.edu.cn (G.D.); wurh651@nenu.edu.cn (W.R.)

² Urban Remote Sensing Application Innovation Center, School of Geographical Sciences, Northeast Normal University, Changchun 130024, China

³ Information Center, Department of Natural and Resources, Changchun 130024, China; charleson@sina.com

⁴ Jilin Agricultural University Institute of Information Technology, Changchun 130024, China; shulingw@jlaue.edu.cn

* Correspondence: zhy@nenu.edu.cn



Citation: Li, H.; Zhang, H.; Li, Q.; Zhao, J.; Guo, X.; Ying, H.; Deng, G.; Rihan, W.; Wang, S. Vegetation Productivity Dynamics in Response to Climate Change and Human Activities under Different Topography and Land Cover in Northeast China. *Remote Sens.* **2021**, *13*, 975. <https://doi.org/10.3390/rs13050975>

Academic Editor: Sang-Eun Park

Received: 21 December 2020

Accepted: 1 March 2021

Published: 4 March 2021

Publisher's Note: MDPI stays neutral with regard to jurisdictional claims in published maps and institutional affiliations.



Copyright: © 2021 by the authors. Licensee MDPI, Basel, Switzerland. This article is an open access article distributed under the terms and conditions of the Creative Commons Attribution (CC BY) license (<https://creativecommons.org/licenses/by/4.0/>).

Abstract: Net primary productivity (NPP) is the total amount of organic matter fixed by plants from the atmosphere through photosynthesis and is susceptible to the influences of climate change and human activities. In this study, we employed actual NPP (ANPP), potential NPP (PNPP), and human activity-induced NPP (HNPP) based on the Hurst exponent and statistical analysis to analyze the characteristics of vegetation productivity dynamics and to evaluate the effects of climate and human factors on vegetation productivity in Northeast China (NEC). The increasing trends in ANPP, PNPP, and HNPP accounted for 81.62%, 94.90%, and 89.63% of the total area, respectively, and ANPP in 68.64% of the total area will continue to increase in the future. Climate change played a leading role in vegetation productivity dynamics, which promoted an increase in ANPP in 71.55% of the area, and precipitation was the key climate factor affecting ANPP. The aggravation of human activities, such as increased livestock numbers and intensified agricultural activities, resulted in a decrease in ANPP in the western grasslands, northern Greater Khingan Mountains, and eastern Songnen Plain. In particular, human activities led to a decrease in ANPP in 53.84% of deciduous needleleaf forests. The impact of climate change and human activities varied significantly under different topography, and the percentage of the ANPP increase due to climate change decreased from 71.13% to 53.9% from plains to urgent slopes; however, the percentage of ANPP increase due to human activities increased from 3.44% to 21.74%, and the effect of human activities on the increase of ANPP was more obvious with increasing slope. At different altitudes, the difference in the effect of these two factors was not significant. The results are significant for understanding the factors influencing the vegetation productivity dynamics in NEC and can provide a reference for governments to implement projects to improve the ecosystem.

Keywords: vegetation productivity dynamics; net primary productivity (NPP); climate change; human activities; Northeast China

1. Introduction

Over the past few decades, global average temperatures have risen by approximately 0.74 °C, and heavy precipitation events will continue to increase in the future [1]. Global climate change has led to significant changes in vegetation respiration, photosynthesis, and the biosphere carbon cycle, which affect ecosystem productivity [2]. In addition, a series of human activities, such as the rapid growth of population and increased industrialization,

have also placed much pressure on ecosystems [3,4]. Accurately evaluating the influences of climate and human factors on ecosystems has great significance for maintaining the sustainable development of ecosystems [5]. However, regional ecosystem changes are often the result of the combination of climate and human factors, and distinguishing the relative influence of the two factors is still a challenge, although it is crucial to understand and manage the landscape [6].

Vegetation is an important part of ecosystems; it plays a key role in regulating ecosystem carbon balance and has the characteristics of adapting to the surface environment and reflecting human activities [4,7]. In recent years, vegetation growth status and surface coverage have undergone dramatic changes in China, and climate and human factors are the main driving forces of vegetation change [8,9]. Because of the continuous development of remote sensing technology, large-area observations and remote sensing analyses of vegetation have become more effective and less costly than human observations [10], and it is easier to obtain remote sensing data to study dynamic trends in vegetation [11–13]. Some studies have used residual trend analysis based on the normalized difference vegetation index (NDVI) to distinguish the effects of human activities on vegetation from other influencing factors [14]. Some studies have used a partial derivative analysis to evaluate the influences of climate and human factors [15]. A multiple linear regression model has also been used to distinguish between the two factors [16]. However, these studies have mainly been based on statistical methods employed to evaluate the relative influences of climate and human factors, ignoring the real ecological significance, which easily leads to uncertainty in the estimation results, and these analyses cannot completely distinguish the impacts of the two factors [17,18].

Net primary productivity (NPP) is the total amount of organic matter fixed by plants from the atmosphere through photosynthesis, and it plays an important role in the carbon cycle of ecosystems [19,20]. NPP is susceptible to the impact of climate and human factors, and the dynamic change in NPP can be used to evaluate the influences of these two factors on vegetation [21]. Accordingly, actual NPP (ANPP) refers to the actual productivity of plants and is influenced by both climate and human factors. Potential NPP (PNPP) represents the NPP value of plants affected by only climate factors, which is an ideal productivity situation. In addition, the result of PNPP minus ANPP can be regarded as NPP affected by human activities (HNPP) [22,23]. By analyzing the trends in ANPP, PNPP, and HNPP at the pixel scale, the relative impacts of the two factors on vegetation can be distinguished [15,18,21]. The method uses NPP to evaluate the influence forces of vegetation productivity change affected by climate and human factors, which is more accurate than statistical analysis methods [24,25].

Northeast China (NEC) is an ecologically sensitive area with rich vegetation resources and diverse topography and has been regarded as one of the most typical warming regions in East Asia [26,27]. In recent years, the temperature in this area has increased, even causing drought [28,29], which will cause vegetation productivity to decrease, changes in vegetation mortality, and ecosystem degradation [30]. Moreover, NEC, as an important crop production base in China, accounts for approximately 20% of China's total grain output. However, the large demand for economic development and food has destroyed a large number of natural land resources, resulting in the loss of biodiversity, water shortages, and other serious ecological consequences [31,32]. Mao et al. [33] found that policies, such as those related to grain production, have a significant impact on land use and ecological carbon storage in NEC. By analyzing the relationship between climate change and vegetation dynamics, Li et al. [29] found that climate change aggravates drought in NEC, and vegetation is at a high risk of drought. However, the relative effects of climate change and human activities on vegetation dynamics in NEC and whether there are differences in the effects of these two factors under different vegetation types and topography remain still unclear. Therefore, it has been very useful to quantitatively assess the impact of human and climate factors on ecosystems in the NEC in recent years.

The objectives of this study are to explore the ANPP spatial distribution and temporal and sustainable trends in NEC; quantify the impact of climate and human factors on ANPP across NEC; and determine the influences of climate and human factors on ANPP under different topography and vegetation types. These research results will provide a basis for government departments to build ecological civilizations and restore ecosystems to enhance ecosystem quality and stability in NEC.

2. Materials and Methods

2.1. Study Area

NEC is located between $38^{\circ}42'–53^{\circ}35'N$ and $115^{\circ}32'–135^{\circ}09'E$, and the area encompasses approximately 1.24 million km^2 [34]. The average elevation is 445 m, covering eastern Inner Mongolia, Liaoning, Jilin, and Heilongjiang provinces (Figure 1a). The annual average temperature is between -1.3 and $6.6^{\circ}C$, and the annual total precipitation is between 500 and 1000 mm [35]. Most of the area has a temperate humid and semi-humid continental monsoon climate, high temperatures, sufficient precipitation, and sunshine in summer, which are conducive to the growth of vegetation. Vegetation types include grass, crops, deciduous broadleaf forests (DBFs), and deciduous needleleaf forests (DNFs), and approximately 37% of the country's forest area is located in NEC. The grass, crops, DBFs, and DNFs in Figure 1a are unchanged vegetation types from 2001 to 2019, and other landcover include areas where landcover has changed, and other landcover types. The terrain of NEC is mainly composed of plains, hills, and mountains, with the Lesser Khingan Mountains located in the north, the Greater Khingan Mountains in the west, and the Changbai Mountains in the east (Figure 1b). Among the mountains is the Northeast Plain, the largest plain in China, which is composed of the Sanjiang Plain, Liaohe Plain, and Songnen Plain. At low altitudes and on the relatively flat plains, human activities are dominated by agricultural activities. For instance, the Songnen Plain and Sanjiang Plain, which are rich in fertile black soil resources, are planted with a large amount of commercial grain and play an important part in grain production in China [36]. In high-altitude areas, such as the Changbai Mountains, due to the high forest coverage and rich material resources, forest resources have been greatly developed and utilized because of the demand for economic development in recent years [27].

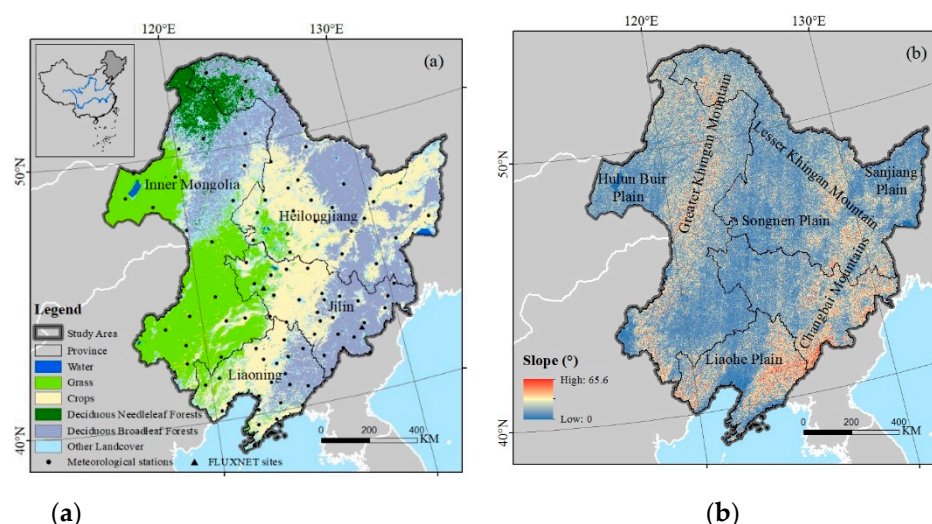


Figure 1. (a) Location of the study area with vegetation types, (b) slope.

2.2. Data Sources

2.2.1. Remote Sensing Data

The 500 m moderate-resolution imaging spectroradiometer (MODIS) NDVI product (MOD13A1) and land cover product (MCD12Q1) were obtained from the Earth Observing

System Data and Information System, National Aeronautics and Space Administration (NASA, <https://ladsweb.modaps.eosdis.nasa.gov> (accessed on 1 March 2021)), and were employed to simulate ANPP. The MOD13A1 NDVI dataset temporal resolution is 16 days, with a time span from 2001 to 2019. The maximum-value composition (MVC) was employed to synthesize monthly datasets from the 16-day MODIS-NDVI products. One of the MCD12Q1 land cover classification schemes, the annual plant functional type (PFT), was used for our study.

2.2.2. Meteorological Data

The monthly average temperature and total precipitation were derived from the China Meteorological Data Sharing Service System (<http://data.cma.cn> (accessed on 1 March 2021)), and NEC includes 107 meteorological stations (Figure 1a). We used ANUSPLIN software combined with digital elevation model (DEM) data to interpolate derived meteorological data, and the station meteorological data were then converted into raster data. The spatial resolution and projection were converted in accordance with the MODIS data.

2.2.3. FLUXNET Data

FLUXNET is a global network for measuring ecosystem fluxes and provides a large amount of data based on eddy covariance measurements, including gross primary productivity (GPP), net ecosystem exchange (NEE), respiration and heat fluxes [37]; the dataset is available at the FLUXNET website (<https://fluxnet.org> (accessed on 1 March 2021)). We used remote sensing data and interpolated meteorological data to calculate simulated ANPP values at the pixel scale, and we extract the pixel values at FLUXNET sites. To verify the accuracy of the simulated ANPP, monthly GPP data from the FLUXNET2015 product were converted to ANPP to compare with the extracted pixel values. Two FLUXNET sites were available in our study area (Figure 1a), including the Changbaishan grassland site, which provides GPP data from 2003 to 2005, and the Changling mixed forest site, which contains GPP data from 2007 to 2010.

2.3. Methods

2.3.1. NPP Estimation

Three types of NPPs were used in this study: ANPP calculated by the Carnegie–Ames–Stanford Approach (CASA) model (Equations (1)–(3)), PNPP calculated by the Thornthwaite Memorial model (Equations (4)–(6)), and HNPP can be calculated through Equation (7).

The CASA model uses NDVI, vegetation types, and meteorological data as input parameters, which are determined by plant absorbed photosynthetically active radiation (APAR) and actual light energy utilization efficiency (ϵ) [38]; this model can be defined as follows:

$$ANPP(x, t) = APAR(x, t) \times \epsilon(x, t) \quad (1)$$

where $APAR(x, t)$ and $\epsilon(x, t)$ can be simulated by the following formulas:

$$APAR(x, t) = SOL(x, t) \times FPAR(x, t) \times 0.5 \quad (2)$$

$$\epsilon(x, t) = T_{\epsilon 1}(x, t) \times T_{\epsilon 2}(x, t) \times W_{\epsilon}(x, t) \times \epsilon_{\max} \quad (3)$$

where $SOL(x, t)$ and $FPAR(x, t)$ represent the total monthly solar radiation (MJ m^{-2}) and the effective radiation absorbed by the plant canopy through photosynthesis, respectively. $T_{\epsilon 1}(x, t)$ and $T_{\epsilon 2}(x, t)$ are the limits of low temperature and high temperature on the utilization of light energy of vegetation, respectively [19]. ϵ_{\max} is the maximum light energy utilization in an ideal state (g C MJ^{-1}). Zhu et al. [39] employed measured ANPP combined with meteorological station data and remote sensing data, and the ϵ_{\max} of typical vegetation in China was calculated. The ϵ_{\max} results were used in this study.

The Thornthwaite Memorial model is built on the basis of the Miami model, which is driven by the relationship among evaporation (ET), temperature, and precipitation [40]. The model was used to calculate PNPP by the following formulas:

$$PNPP = 3000 \left[1 - e^{-0.0009695(v-20)} \right] \quad (4)$$

$$v = \frac{1.05r}{\sqrt{1 + \left(1 + \frac{1.05r}{L} \right)^2}} \quad (5)$$

$$L = 3000 + 25t + 0.05t^3 \quad (6)$$

where v and L represent actual and mean evapotranspiration (mm), respectively. t and r are the annual mean temperature ($^{\circ}\text{C}$) and total precipitation (mm), respectively.

HNPP reflects the loss of vegetation productivity affected by human activities and can be simulated by the following formula [24]:

$$HNPP = PNPP - ANPP \quad (7)$$

2.3.2. R/S Analysis

R/S analysis is the most widely used method to calculate the Hurst exponent. British hydrologist Hurst first came up with the Hurst exponent, and R/S analysis can effectively evaluate the correlation of long time series, which can be used for future trend analysis [41]. R/S analysis can be conducted through Equations (8)–(12).

The long time series $\{\xi(\tau)\}$ can be divided into τ subsequences, and the average value for each sequence was defined as follows:

$$\langle \xi \rangle_{\tau} = \frac{1}{\tau} \sum_{t=1}^{\tau} \xi(t), \tau = 1, 2, \dots \quad (8)$$

The accumulated deviation for each sequence was calculated as follows:

$$X(t, \tau) = \sum_{u=1}^t [\xi(u) - \langle \xi \rangle_{\tau}], 1 \leq t \leq \tau. \quad (9)$$

The range sequence was calculated as follows:

$$R(\tau) = \max_{1 \leq t \leq \tau} X(t, \tau) - \min_{1 \leq t \leq \tau} X(t, \tau), \tau = 1, 2, \dots \quad (10)$$

The standard deviation sequence was defined as follows:

$$S(\tau) = \left[\frac{1}{\tau} \sum_{t=1}^{\tau} (\xi(t) - \langle \xi \rangle_{\tau})^2 \right]^{\frac{1}{2}}, \tau = 1, 2, \dots \quad (11)$$

The Hurst exponent H can be defined by R , S , and τ as follows:

$$R(\tau) / S(\tau) = c \cdot \tau^H \quad (12)$$

where c is a constant. According to Wang [10], the Hurst exponent index ranges from 0 to 1 and indicates three states. When $0 < H < 0.5$, changes in the time series were inconsistent, and the sequence may have an opposite trend in the future. When H equals 0.5, changes in the time series were stochastic, and the trend in the past had no effect on the future. When $0.5 < H < 1$, changes in the time series were consistent, and the future had the same trend as the past. The closer H was to 0, the more inconsistent the time series was; in contrast, the closer H was to 1, the more consistent the sequence was. According to the classification method based on the Hurst index [42], we defined strong inconsistency of time series as H

less than 0.25, weak inconsistency for H from 0.25 to 0.5, weak consistency for H from 0.5 to 0.75, and strong consistency for H greater than 0.75.

2.3.3. Partial Correlation Analysis

Partial correlation analysis was employed to evaluate the relationship between ANPP and climate factors. This method removes the influence of other related variables, so it can effectively evaluate the correlation between two variables [43] and is calculated through Equation (13):

$$R_{xy,z} = \frac{R_{xy} - R_{xz} \cdot R_{yz}}{\sqrt{(1 - R_{xz}^2) \cdot (1 - R_{yz}^2)}} \quad (13)$$

where $R_{xy,z}$ is the partial correlation coefficient between x and y while removing the influence of the variable z . R_{xy} , R_{xz} , and R_{yz} are the Pearson correlation coefficients between two variables. In addition, the t -test was employed to demonstrate the significance of the correlation.

2.3.4. Convert GPP to NPP

The conversion formula of eddy covariance measured gross primary productivity to NPP is described as Equation (14) [44]:

$$NPP = CUE \cdot GPP \quad (14)$$

where CUE is the carbon use efficiency. Previous studies have argued that CUE is constant [45,46]. Waring et al. [47] suggested that most forest CUE has a uniform value of 0.47, while Liu et al. [44] found that the CUE values of grassland range from 0.48 to 0.56. In this study, because the vegetation types of the two FLUXNET sites are grassland and mixed forest, we set CUE to 0.5 to calculate the FLUXNET site-observed ANPPs.

3. Results

3.1. Validation of Simulated ANPP

We extracted the CASA-simulated monthly ANPP values from the two FLUXNET sites of Changbaishan and Changling. Figure 2 shows the comparison of the extracted CASA-simulated ANPP with the FLUXNET site-observed ANPPs. The significant correlation ($R^2 = 0.93$, $p < 0.001$) demonstrated that the simulated results are accurate.

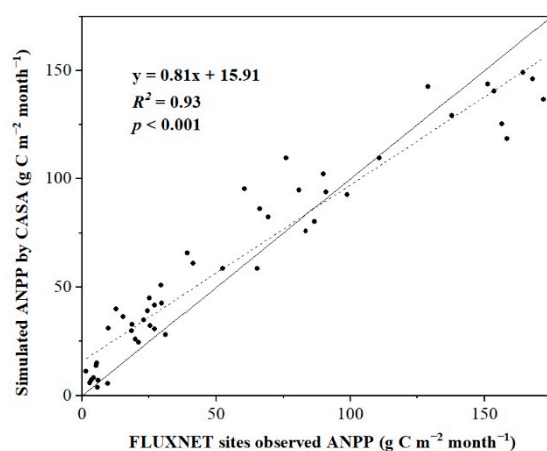


Figure 2. Comparison of actual net primary productivity (ANPP) simulated by Carnegie–Ames–Stanford Approach (CASA) model with FLUXNET site-observed ANPPs.

3.2. Spatial Characteristics of NPP from 2001 to 2019

3.2.1. Spatial Distribution of ANPP

Figure 3 shows the spatial distribution of the mean ANPP in NEC, and the average ANPP was $477.90 \text{ g C m}^{-2} \text{ year}^{-1}$ during 2001–2019. High values of ANPP appeared in the region of the Changbai Mountains, Greater Khingan Mountains, and Lesser Khingan Mountains, and low values were observed in the Hulun Buir Plain and Songnen Plain. According to vegetation type, the largest average ANPP was $638.34 \text{ g C m}^{-2} \text{ year}^{-1}$ for DBF, followed by cropland at $456.43 \text{ g C m}^{-2} \text{ year}^{-1}$, DNF at $354.55 \text{ g C m}^{-2} \text{ year}^{-1}$, and grassland at $347.18 \text{ g C m}^{-2} \text{ year}^{-1}$.

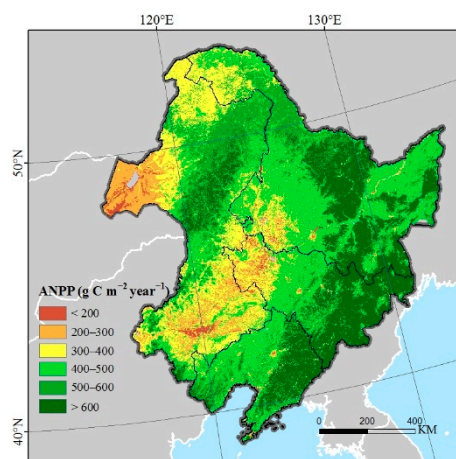


Figure 3. Spatial distribution of the average ANPP in Northeast China (NEC) during 2001–2019.

3.2.2. ANPP, PNPP and HNPP Trends

The ANPP in most regions of NEC presented an increasing trend (Figure 4a), with a mean increment of $2.29 \text{ g C m}^{-2} \text{ year}^{-1}$ during 2001–2019. The increasing region accounted for 81.62% of the study area, while the decreasing trend area was rare (18.38% of the study area) and was distributed across the eastern Sanjiang Plain, southern Liaohe Plain, and DNF area. Figure 4b shows the spatial distribution of the Hurst exponent of ANPP; 83.43% of the study area was consistent with the current state, among which strong consistency and weak consistency accounted for 40.88% and 42.55%, respectively. Only 16.57% of the total area ANPP was the opposite of the current state, and strong inconsistency and weak inconsistency accounted for 4.04% and 12.53%, respectively. We spatially overlaid Figure 4a,b, and we combined the attributes of the two layers at the pixel scale to obtain Figure 4c. The result shows that 68.64% of the total area had a continuous increasing trend in the future, only 14.79% of the study area showed a continuous decreasing trend, 3.59% of the area converted from decreasing to increasing, and 12.98% converted from increasing to decreasing. The results indicate that the ANPP in 72.23% of NEC will increase, and the ANPP of different vegetation types is dominated by a future increase. However, DNF had the largest areal decrease in ANPP in the future (48.19% of the DNF area).

Figure 5a,b show the spatial PNPP and HNPP trends in NEC during 2001–2019, and the areas of PNPP and HNPP with positive trends accounted for 94.90% and 89.63% of the total area, respectively. A positive PNPP trend indicates that climate change promotes vegetation productivity, and a positive HNPP trend indicates that human activities reduce the productivity of vegetation. In the southern Changbai Mountains, human activities had a promotional effect, and climate change had a negative impact on vegetation productivity, and most trends in HNPP in this region were below -5 (Figure 5b), while the trends in PNPP were mainly between -5 and 0 ; the decreasing rate of HNPP was greater than that of PNPP, which suggests that the restoration effect of human activities on vegetation productivity was larger than the reduction effect of climate change. Therefore, ANPP remained dominated by an increase in this area (Figure 4a).

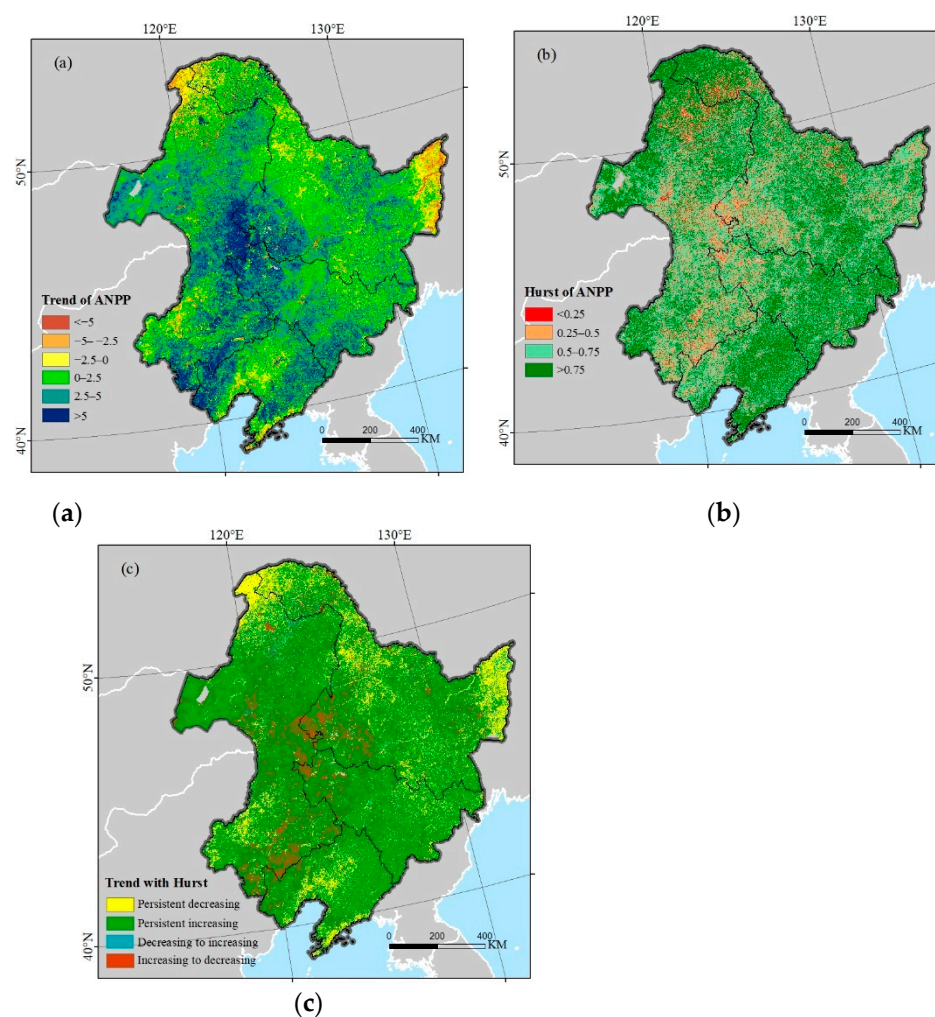


Figure 4. (a) Trend of ANPP, (b) Hurst exponent of ANPP, and (c) trend with Hurst in NEC during 2001–2019.

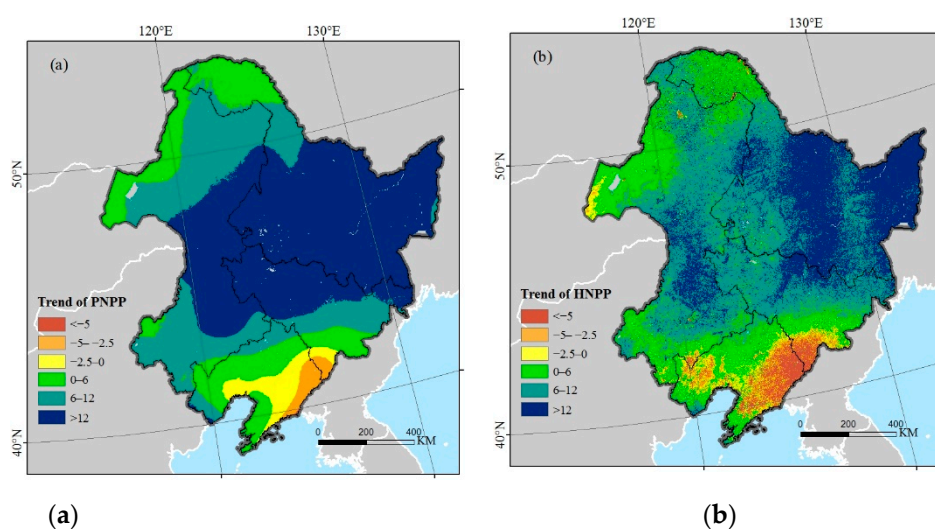


Figure 5. (a) potential NPP (PNPP) and (b) human activity-induced NPP (HNPP) trends in NEC during 2001–2019.

3.3. Relative Influences of Climate Change and Human Activities on Vegetation Productivity

3.3.1. Influences of Climate Change and Human Activity on Vegetation ANPP Dynamics

According to the classification method in Table 1, the influences of climate and human factors on ANPP were divided into six scenarios. Figure 6 shows the spatial distribution of the classification results. Climate change was the leading factor affecting the increase in ANPP, accounting for 71.55% of the study area, which was located in the middle of NEC. Human activities (4.28% of the area) and the combination of two factors (5.79% of the area) induced a reduced increase in ANPP and were distributed in the southern Changbai Mountains. Human activities were the main factor affecting the decrease in ANPP, accounting for 17.56% of the study area and being located in the DNF area and Sangjiang Plain. Climate change (0.3% of the area) and the combination of two factors (0.52% of the area) induced a reduced decrease in ANPP.

Table 1. Six scenarios for evaluating the driving factors of ANPP in NEC [17,18]. SANPP, SPNPP, and SHNPP represent the slopes of ANPP, PNPP, and HNPP during 2001–2019, respectively.

SANPP	SPNPP	SHNPP	Driving Factors of ANPP
+	+	+	Increase due to climate change (IDC)
+	—	—	Increase due to human activities (IDH)
+	+	—	Increase due to the combined influences of climate change and human activities (IDCH)
—	—	—	Decrease due to climate change (DDC)
—	+	+	Decrease due to human activities (DDH)
—	—	+	Decrease due to the combined influences of climate change and human activities (DDCH)

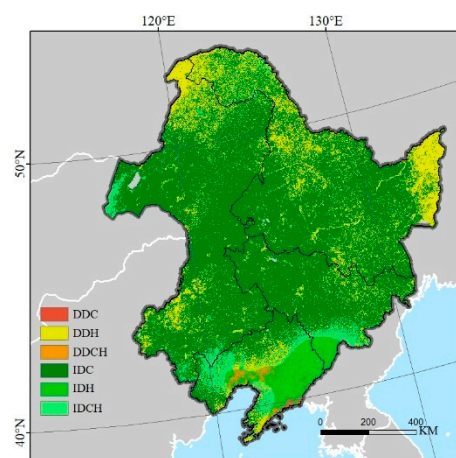


Figure 6. Spatial distribution of the influences of climate and human factors on vegetation productivity in NEC. See Table 1 for the definitions of the driving forces.

3.3.2. Analysis of Driving Factors for Different Vegetation Types

Figure 7a shows the area percentage of ANPP increase affected by climate and human factors for different vegetation types. To avoid the impact of land cover type change, we selected the area where grass, crops, DNF, and DBF did not change from 2001 to 2019. Climate change is the major factor affecting the increase in ANPP and had the largest effect on grassland, accounting for 82.53% of grassland area. Moreover, 75.24% of the cropland area and 68.25% of the DBF area showed an increase in ANPP due to climate change, and climate change had the lowest influence on DNF, accounting for 45.55% of the DNF area. Figure 7b shows the area percentage of ANPP decrease affected by climate and human factors for different vegetation types, and human activities were the major driving force affecting the decrease in ANPP for different vegetation types. Human activities led to 53.84% of the DNF area ANPP decrease, and the percentages of DBF, cropland, and

grassland were 17.71%, 16.15%, and 9.48%, respectively. The combination of the two factors had less of an impact on ANPP. In conclusion, climate change was the major factor leading to the ANPP increase, and human activities were the leading factor affecting the ANPP decrease for different vegetation types. Compared with other vegetation types, DNF was more sensitive to human activities.

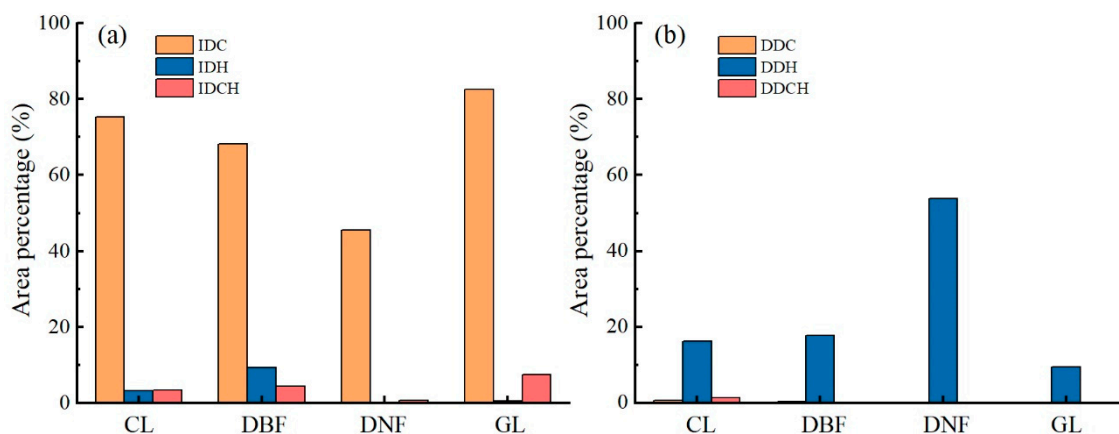


Figure 7. Area percentage of ANPP (a) increase and (b) decrease affected by climate and human factors for different vegetation types. CL: cropland; DBF: deciduous broadleaf forest; DNF: deciduous needleleaf forest; and GL: grassland. See Table 1 for the definitions of the driving forces.

Based on the vegetation types of NEC in 2001, we extracted the stable change areas of vegetation types through the landcover data in 2009 and 2019. Through the analysis of vegetation types change in NEC (Table 2), we found that grassland accounted for the largest proportion of land-use change, and 10.8% of grassland changed into crops, which indicated that the intensification of human agricultural activities was one of the reasons for grassland degradation in this region. According to Table 2, 14.37% of DNF was converted into other land use types, while the conversion of other land use types into DNF was rare, indicating that DNF has been further degraded due to recent land-use changes.

Table 2. Area (unit: 10^3 m^2) and percentage of land cover change in NEC from 2001 to 2019. DNF: deciduous needleleaf forest; DBF: deciduous broadleaf forest.

Land Cover	Area	Translates to											
		Grass		Crop		DNF		DBF		Others		Change	
		Area	%	Area	%	Area	%	Area	%	Area	%	Area	%
Grass	362.67	301.21	83.05	39.13	10.80	0.69	0.19	20.29	5.59	1.35	0.37	61.46	16.95
Crops	390.11	15.01	3.85	354.41	90.85	0.03	0.00	19.30	4.95	1.36	0.35	35.70	9.15
DNF	74.30	0.72	0.97	0.01	0.00	63.62	85.63	9.75	13.12	0.20	0.28	10.68	14.37
DBF	388.56	7.15	2.35	6.00	1.54	9.73	2.50	363.46	93.54	0.22	0.07	25.1	6.46

3.3.3. Analysis of the Driving Factors in Different Topographic Elements

We graded the altitude and slope according to the International Geographical Union Commission on Geomorphological Survey and Mapping to explore the driving factors affecting the vegetation productivity dynamics in different topographic elements in NEC. The different altitudes can be divided into plains ($\leq 200 \text{ m}$), hills ($200\sim 500 \text{ m}$), low mountains ($500\sim 1000 \text{ m}$), and high mountains ($>1000 \text{ m}$). Table 3 shows that the average ANPP of high mountains was the largest at $511.04 \text{ g C m}^{-2} \text{ year}^{-1}$. Approximately 63.73% of cropland was distributed in the plains, DNF was mainly distributed in the low mountains (76.36% of the area), and DBF and grassland were mainly distributed in the hills and low mountains. According to Table 3, the average area percentages of IDC and IDH at different

altitudes were 71.12% and 3.56%, respectively. Therefore, at different altitudes, climate change was the leading factor affecting the increase in vegetation ANPP. The average area percentages of DDC and DDH at different altitudes were 0.27% and 18.51%, respectively; thus, human activities were the main factor affecting the decrease in vegetation ANPP. The effects had no obvious distinctions for different altitude grades.

Table 3. Effects of different altitudes on the mean ANPP (unit: $\text{g C m}^{-2} \text{ year}^{-1}$), vegetation type distribution and driving forces in NEC. CL: cropland; DBF: deciduous broadleaf forest; DNF: deciduous needleleaf forest; and GL: grassland. See Table 1 for definitions of the driving forces.

Altitude (m)	Mean ANPP	Area Percentage (%)				Influence Factors (%)						
		CL	DBF	DNF	GL	IDC	IDH	IDCH	DDC	DDH	DDCH	Total
≤200	432.22	63.73	5.1	0.39	19.12	70.78	4.7	3.63	0.83	18.37	1.69	100
200~500	509.81	32.69	46.88	9.05	24.3	73.31	5.01	5.2	0.16	16.2	0.12	100
500~1000	484.24	3.33	42.01	76.36	46.65	70.56	3.75	8.16	0.05	17.46	0.02	100
>1000	511.04	0.25	6.01	14.2	9.93	69.81	0.77	7.39	0.02	22	0.01	100
Total		100	100	100	100							100

Grading according to slope, the study area can be divided into plains ($\leq 2^\circ$), gentle slopes ($2\sim 5^\circ$), inclined slopes ($5\sim 15^\circ$), steep slopes ($15\sim 25^\circ$), and urgent slopes ($>25^\circ$). ANPP increased with increasing slope grade (Table 4), the mean ANPP of the plains was the lowest ($421.09 \text{ g C m}^{-2} \text{ year}^{-1}$), and the mean ANPP on the urgent slopes was the largest ($611.09 \text{ g C m}^{-2} \text{ year}^{-1}$). All vegetation types had the largest area percentage on inclined slopes, and the percentages of cropland, DBF, DNF, and grassland were 46.1%, 51.62%, 55.82%, and 45.39%, respectively. At different slope grades, the average area percentages of IDC and IDH were 67.41% and 7.01%, respectively; thus, climate change was the major factor affecting the increase in ANPP. The average area percentages of DDC and DDH under different slope grades were 0.42% and 16.60%, respectively; thus, human activities led to a decrease in ANPP. With increasing slope grade, the area percentage of the ANPP driving factors also changed, and the percentage of the increase in ANPP due to climate change decreased from 71.13% to 53.9%; however, the percentage of the increase in ANPP due to human activities increased from 3.44% to 21.74%. The results showed that as the slope increased, the influence of human activities on the increase in ANPP also increased.

Table 4. Effects of different slopes on the mean ANPP (unit: $\text{g C m}^{-2} \text{ year}^{-1}$), vegetation type distribution and driving forces in NEC. CL: cropland; DBF: deciduous broadleaf forest; DNF: deciduous needleleaf forest; and GL: grassland. See Table 1 for definitions of the driving forces.

Slope (°)	Mean ANPP	Area Percentage (%)				Influence Factors (%)						
		CL	DBF	DNF	GL	IDC	IDH	IDCH	DDC	DDH	DDCH	Total
≤2	421.09	13.05	3.87	3.87	11.61	71.13	3.44	4.33	0.74	18.72	1.64	100
2~5	434.80	35.52	15.88	16.57	33.22	74.65	1.91	4.04	0.32	18.4	0.68	100
5~15	484.53	46.1	51.62	55.82	45.39	72.78	3.05	5.96	0.19	17.71	0.31	100
15~25	572.38	4.71	22.32	19.23	7.98	64.59	10.57	8.83	0.31	15.43	0.27	100
>25	611.09	0.62	6.31	4.51	1.8	53.9	21.74	10.76	0.55	12.74	0.31	100
Total		100	100	100	100							100

3.4. The Relationship between Vegetation ANPP and Climate Factors

The average partial correlation coefficient between vegetation ANPP and temperature was 0.15 in NEC. The area of positive correlation accounted for 71.87% of the study area (Figure 8a), and there was a significant positive correlation ($p < 0.05$) in 10.83% of the area, which was distributed in the central NEC. Twenty-eight percent of the study area presented a negative correlation between ANPP and temperature, which was distributed in grassland

and deciduous forest regions of western NEC, and only 0.54% passed the significance test. The average partial correlation coefficient between vegetation ANPP and precipitation in the study area was 0.38, and 89.22% of the study area was positively correlated (Figure 8b); 42.21% of the area passed the significance test and was mainly distributed in grassland and cropland in the western part of NEC. ANPP in 10% of the study area was negatively correlated with precipitation, and this area was mainly located in the Greater Khingan Mountains and Changbai Mountains; only 0.41% passed the significance test.

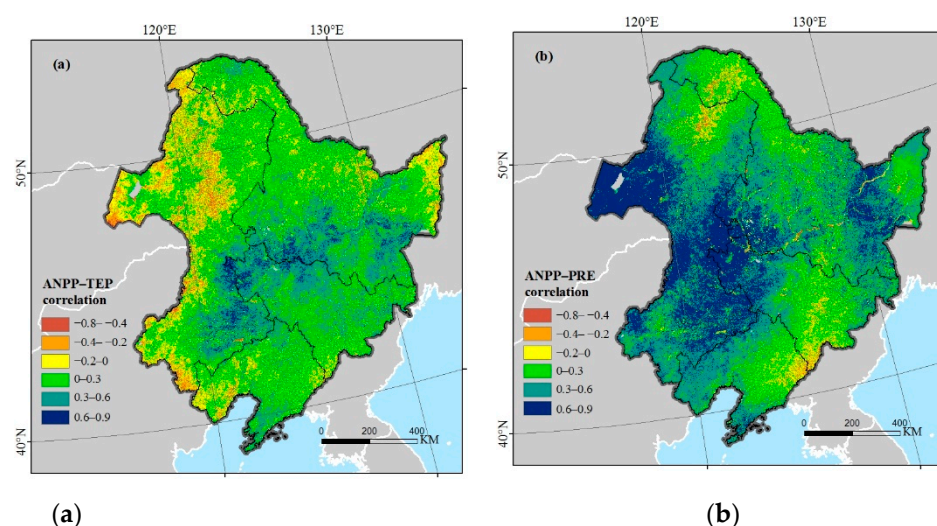


Figure 8. Spatial distribution of partial correlation coefficients between (a) ANPP and annual average temperature and (b) ANPP and annual total precipitation.

4. Discussion

4.1. ANPP Change Characteristics in NEC

The ANPP in 81.62% of the NEC area had a tendency to increase due to climate and human factors from 2001 to 2019 (Figure 4a). Zeng et al. [48] also noted that NEC vegetation restoration was significant from 2000 to 2015. The Hurst exponent in NEC showed that except for some grassland, Sanjiang Plain, and DNF areas, the ANPP will continue to increase in most regions in the future (Figure 4c). Changes in temperature and precipitation can affect vegetation growth and increases in ANPP will benefit from global warming [49]. Increasing heat resources brought about by global warming will increase crop yield in most of the crop-producing areas in NEC [50]. In addition to climate change, changes in atmospheric CO₂ will also affect vegetation productivity. With the increase in global warming and atmospheric CO₂ content in the future, plant photosynthesis is promoted, and respiration is inhibited, leading to an increase in vegetation ANPP [51].

4.2. Role of Climate Change in Determining ANPP

Spatially, 71.55% of the study area ANPP increased due to climate change (Figure 6), and most of the areal ANPP was positively correlated with climatic factors (temperature and precipitation) (Figure 8ab). Vegetation productivity changes have been associated with climate change in different ecosystems over the past decades, especially temperature and precipitation factors [52,53]. Climate change can impact ecosystem productivity by changing the surface water content and soil organic matter and affecting vegetation respiration and photosynthesis [54]. The mean partial correlation coefficient between ANPP and temperature in the entire study area was 0.15, and negative correlations were mainly distributed in grassland and DBF areas in the Inner Mongolia region (Figure 8a). There is less precipitation in this area, and as the temperature rises, vegetation growth will be restrained. In the past 50 years, Inner Mongolia has become a warmer and drier region [55]. Although a temperature rise can increase the plant photosynthesis and respiration rates, temperature will have a negative effect if the temperature is too high to exceed the limita-

tion [56]. Warming without more precipitation may aggravate the impact of drought on the environment, which will have adverse effects on plant growth [8,57]. Therefore, ANPP was negatively correlated with temperature in the relatively arid Inner Mongolia region, while the eastern region with more precipitation exhibited a positive correlation.

ANPP was positively correlated with precipitation in a total of 89.22% of the study area (Figure 8b), and the average correlation coefficient was 0.38. Compared with temperature, the effect of precipitation on ANPP was stronger in NEC. Precipitation is often considered to be the leading factor for vegetation growth because water shortages may lead to many limitations of vegetation, which will severely restrict the growth of vegetation [8,58]. ANPP was significantly positively correlated with precipitation in the western grassland, which may be because increasing precipitation can increase grassland coverage [7], and grassland productivity is improved. The correlation between precipitation and vegetation ANPP is weak in the north and east of NEC, even with a negative correlation in the Changbai Mountains and northern Greater Khingan Mountains. Mao et al. [34] also observed that the NDVI in the Lesser Khingan Mountains and Changbai Mountains was negatively correlated with precipitation. These regions have cold and snowy springs, and precipitation will lead to more clouds, thus reducing incident radiation [34]. The decrease in incident radiation will weaken photosynthesis and affect the growth of vegetation [59]. The decrease in photosynthesis reduced carbon sequestration in plants; therefore, there was a negative correlation between ANPP and precipitation.

4.3. Role of Human Activities in Determining ANPP

In recent years, the Chinese government has carried out many ecological projects to protect vegetation ecosystems. With the implementation of multiple afforestation programs, such as the Grain to Green Program (GTGP), the vegetation in NEC has experienced accelerated greening due to human activity [60]. The natural forest conservation project (NFCP) and GTGP had obvious effects on woodlands, and the implementation of ecological protection projects resulted in a total 2256 km² increase in woodlands after 2000 in NEC [33]. Topography is also an important factor affecting vegetation growth on a large spatial scale [61]. Slope can affect surface runoff, soil water content, and other physico-chemical properties, leading to changes in the vegetation growth environment [62]. The GTGP program explicitly forbids reclamation in areas with slopes over 25°; in addition, exploitation on slopes between 15° and 25° is not recommended [21]. Our results showed that the region with an increase in ANPP caused by human activities was mainly distributed in the Changbai Mountains in the southern NEC area (Figure 6), where the slope is steep (Figure 1b). According to Table 4, with the increase in slope, the contribution rate of human factors to the increase in ANPP also increased. Therefore, our results indirectly prove the effectiveness of the GTGP in NEC.

The decrease in ANPP caused by human factors is distributed in the western Inner Mongolia grassland, the Sanjiang Plain, and northern DNFs (Figure 6). Grassland degradation in Inner Mongolia can be caused by overgrazing. According to the Statistics Bureau of Inner Mongolia (<http://tj.nmg.gov.cn> (accessed on 1 March 2021)), the total amount of livestock in four Inner Mongolian cities in NEC increased significantly (Figure 9a), resulting in the consumption of grassland plant biomass increasing and grassland degradation accelerating [19]. If the number of livestock exceeds the capacity of grassland ecosystems, this will reduce the resilience of grassland and cause grassland degradation [21]. Therefore, it is necessary to control the livestock volume in Inner Mongolia to improve the grassland ecological environment. The ANPP decrease in the DNF area in Greater Khingan caused by human activities was more intense than that in other vegetation types (Figure 7b), which may be related to the frequent occurrence of forest fires in this area. Forest fires have occurred frequently in this region in recent years, and the average annual burnt area of the DNF area extracted from MODIS (MCD64A1) is 3210 ha (Figure 9b). Some studies have found that fires in boreal forests in NEC are closely related to human activities, and fire sites are close to residential areas and roads [63]. With global warming, the forest fire

risk level in this area will also increase in the future [64], which should be given more research focus.

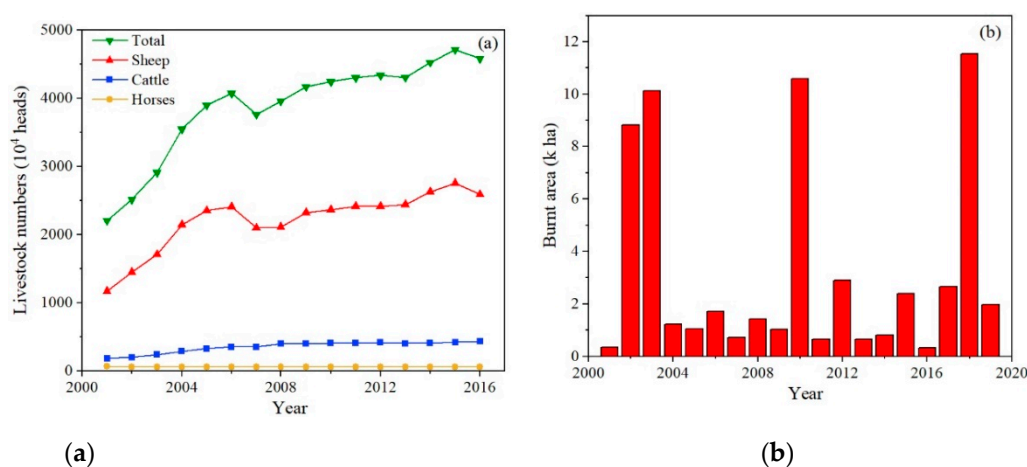


Figure 9. (a) Interannual variations in livestock numbers in four Inner Mongolian cities in NEC (one cattle or horse is regarded to be the same as four sheep) and (b) annual burning area of the DNF area.

The change in land use and land cover caused by human activities can also affect the dynamics of vegetation [65], and land-use changes have a great impact on carbon sequestration [66]. During the study period, landcover changed significantly in NEC, and 10.8% of grassland changed into crops (Table 2). Due to the economic development under the influence of policy in NEC, the demand for land use has increased, which makes the large-scale grassland transformed into crops, resulting in the continuous expansion of crop area in recent years [67]. Furthermore, numerous marshland regions have been reclaimed as cropland over the past 30 years across the Sanjiang Plain, leading to aggravated fragmentation of marshlands [68,69]. The conversion of marshlands to cropland accelerated the decomposition of topsoil organic matter, resulting in soil organic carbon loss [70]. Therefore, the intensification of human agricultural activities may lead to a decrease in the ANPP over the Sanjiang Plain.

4.4. Limitations of This Study

In this study, we employed a methodology using ANPP, PNPP, and HNPP as parameters to quantitatively evaluate the influences of climate and human factors on ANPP in NEC. In addition, the limitations of our study should also be noted. First, the Thornthwaite Memorial model for calculating PNPP only considers the climate factors of temperature and precipitation and does not consider solar radiation, while solar radiation is also one of the meteorological factors affecting NPP [71]. In addition, PNPP is the NPP value that is completely unaffected by human beings and was not verified with measured data in this study; thus, there was uncertainty in the simulated PNPP. Second, human activities, such as fire and land-use change, can affect vegetation productivity dynamics. However, this study only quantitatively discusses the influence of human activities. Because of the limitations of our methodology, these human factors cannot be quantified, which is also a great challenge for future research. Finally, we resampled the interpolated meteorological images to 500 m to keep the spatial resolution consistent with MODIS, which sacrifices pixel accuracy to some extent. Although there are some shortcomings in the evaluation method, the results can reflect the overall change trend in ANPP and the relative impact of climate and human factors on a large scale in NEC, and the results are valuable for policymaking and further research.

5. Conclusions

Based on three NPP indices (ANPP, PNPP, and HNPP) simulated by meteorological data and remote sensing data, we quantitatively discussed the influences of climate change and human activities on ANPP in NEC. The findings are described as follows:

- The average ANPP of the entire study area was $477.90 \text{ g C m}^{-2} \text{ year}^{-1}$ from 2001 to 2019, the area of increased ANPP accounted for 81.62% of NEC, and the area of decreased ANPP was mainly distributed across the eastern Sanjiang Plain, southern Liaohe Plain, and DNFs. According to the analysis of the Hurst exponent, the ANPP change exhibited a certain sustainability, and the ANPP in 72.23% of the study area will increase in the future.
- Compared with human activities, climate change has a greater influence on ANPP, which promoted the increase in ANPP in 71.55% of the study area. In addition, the influences of climate factors (temperature and precipitation) on ANPP have spatial differences. ANPP in the western part of the study area was negatively correlated with temperature because of less precipitation. ANPP was negatively correlated with precipitation in the Greater Khingan Mountains and Changbai Mountains. In the western grasslands, northern Greater Khingan Mountains, and eastern Songnen Plain, ANPP decreased with intensified human activities. In the southern Changbai Mountains, ANPP increased due to human activities.
- Compared with other vegetation types, DNF was most affected by human activities, and ANPP in 53.84% of the DNF area decreased because of human activities. In different topography, the impact of human activities on vegetation productivity was also different; with increasing slope, the contribution rate of human activities to the increase in ANPP also increased, while the effects had no obvious distinction at different altitude grades.

Author Contributions: Conceptualization, H.L. and H.Z.; methodology, H.L. and X.G.; software, Q.L. and G.D.; validation, H.Y., W.R. and S.W.; investigation, J.Z.; data curation, X.G. and J.Z.; writing—review and editing, H.L. and H.Z. All authors have read and agreed to the published version of the manuscript.

Funding: This research was funded by the National Natural Science Foundation of China (Grant No. 41871330 and 41771450), the Fundamental Research Funds for the Central Universities (Grant No. 2412019FZ002 and 2412019BJ001), and the Science and Technology Development Project of Jilin Province (Grant No. 20180623058TC, 20190103151JH and 20190802024ZG).

Institutional Review Board Statement: Not applicable.

Informed Consent Statement: Not applicable.

Data Availability Statement: The data presented in the paper are available from the corresponding author.

Acknowledgments: The authors would like to thank the Key Laboratory of Geographical Processes and Ecological Security in Changbai Mountains, Ministry of Education, and Urban Remote Sensing Application Innovation Center, School of Geographical Sciences, Northeast Normal University for supporting this research. The authors would also like to thank two anonymous reviewers and editors for their constructive comments.

Conflicts of Interest: The authors declare no conflict of interest.

References

1. Intergovernmental Panel on Climate Change. *Climate Change 2013: The Physical Science Basis. Contribution of Working Group I to the Fifth Assessment Report of the Intergovernmental Panel on Climate Change*; Cambridge University Press: Cambridge, UK; New York, NY, USA, 2013.
2. Zhao, M.; Running, S.W. Drought-Induced Reduction in Global Terrestrial Net Primary Production from 2000 Through 2009. *Science* **2010**, *329*, 940–943. [[CrossRef](#)]
3. Cumming, G.S.; Buerkert, A.; Hoffmann, E.M.; Schlecht, E.; von Cramon-Taubadel, S.; Tschardtke, T. Implications of agricultural transitions and urbanization for ecosystem services. *Nature* **2014**, *515*, 50–57. [[CrossRef](#)] [[PubMed](#)]

4. Newbold, T.; Hudson, L.N.; Hill, S.L.L.; Contu, S.; Lysenko, I.; Senior, R.A.; Boerger, L.; Bennett, D.J.; Choimes, A.; Collen, B.; et al. Global effects of land use on local terrestrial biodiversity. *Nature* **2015**, *520*, 45–50. [\[CrossRef\]](#)
5. Dirnbock, T.; Dullinger, S.; Grabherr, G. A regional impact assessment of climate and land-use change on alpine vegetation. *J. Biogeogr.* **2003**, *30*, 401–417. [\[CrossRef\]](#)
6. Ye, X.; Zhang, Q.; Liu, J.; Li, X.; Xu, C. Distinguishing the relative impacts of climate change and human activities on variation of streamflow in the Poyang Lake catchment, China. *J. Hydrol.* **2013**, *494*, 83–95. [\[CrossRef\]](#)
7. Li, C.; Qi, J.; Yang, L.; Wang, S.; Yang, W.; Zhu, G.; Zou, S.; Zhang, F. Regional vegetation dynamics and its response to climate change—A case study in the Tao River Basin in Northwestern China. *Environ. Res. Lett.* **2014**, *9*, 125003. [\[CrossRef\]](#)
8. Liu, Y.; Zhang, Z.; Tong, L.; Khalifa, M.; Wang, Q.; Gang, C.; Wang, Z.; Li, J.; Sun, Z. Assessing the effects of climate variation and human activities on grassland degradation and restoration across the globe. *Ecol. Indic.* **2019**, *106*, 105504. [\[CrossRef\]](#)
9. Wang, H.; Sun, B.; Yu, X.; Xin, Z.; Jia, G. The driver-pattern-effect connection of vegetation dynamics in the transition area between semi-arid and semi-humid northern China. *Catena* **2020**, *194*, 104713. [\[CrossRef\]](#)
10. Wang, B.; Xu, G.; Li, P.; Li, Z.; Zhang, Y.; Cheng, Y.; Jia, L.; Zhang, J. Vegetation dynamics and their relationships with climatic factors in the Qinling Mountains of China. *Ecol. Indic.* **2020**, *108*, 105719. [\[CrossRef\]](#)
11. Huete, A. Ecology: Vegetation's responses to climate variability. *Nature* **2016**, *531*, 181–182. [\[CrossRef\]](#)
12. Deng, G.; Zhang, H.; Guo, X.; Shan, Y.; Ying, H.; Rihan, W.; Li, H.; Han, Y. Asymmetric Effects of Daytime and Nighttime Warming on Boreal Forest Spring Phenology. *Remote Sens.* **2019**, *11*, 1651. [\[CrossRef\]](#)
13. Wang, C.; Jiang, Q.o.; Deng, X.; Lv, K.; Zhang, Z. Spatio-Temporal Evolution, Future Trend and Phenology Regularity of Net Primary Productivity of Forests in Northeast China. *Remote Sens.* **2020**, *12*, 3670. [\[CrossRef\]](#)
14. Li, A.; Wu, J.; Huang, J. Distinguishing between human-induced and climate-driven vegetation changes: A critical application of RESTREND in inner Mongolia. *Landsc. Ecol.* **2012**, *27*, 969–982. [\[CrossRef\]](#)
15. Zhang, Y.; Zhang, C.; Wang, Z.; Chen, Y.; Gang, C.; An, R.; Li, J. Vegetation dynamics and its driving forces from climate change and human activities in the Three-River Source Region, China from 1982 to 2012. *Sci. Total Environ.* **2016**, *563*, 210–220. [\[CrossRef\]](#) [\[PubMed\]](#)
16. Li, D.; Xu, D.; Wang, Z.; You, X.; Zhang, X.; Song, A. The dynamics of sand-stabilization services in Inner Mongolia, China from 1981 to 2010 and its relationship with climate change and human activities. *Ecol. Indic.* **2018**, *88*, 351–360. [\[CrossRef\]](#)
17. Chen, T.; Bao, A.; Jiapaer, G.; Guo, H.; Zheng, G.; Jiang, L.; Chang, C.; Tuerhanjiang, L. Disentangling the relative impacts of climate change and human activities on arid and semiarid grasslands in Central Asia during 1982–2015. *Sci. Total Environ.* **2019**, *653*, 1311–1325. [\[CrossRef\]](#)
18. Chen, B.; Zhang, X.; Tao, J.; Wu, J.; Wang, J.; Shi, P.; Zhang, Y.; Yu, C. The impact of climate change and anthropogenic activities on alpine grassland over the Qinghai-Tibet Plateau. *Agric. For. Meteorol.* **2014**, *189*, 11–18. [\[CrossRef\]](#)
19. Mu, S.; Zhou, S.; Chen, Y.; Li, J.; Ju, W.; Odeh, I.O.A. Assessing the impact of restoration-induced land conversion and management alternatives on net primary productivity in Inner Mongolian grassland, China. *Glob. Planet. Change* **2013**, *108*, 29–41. [\[CrossRef\]](#)
20. Zhang, F.; Zhang, Z.; Kong, R.; Chang, J.; Tian, J.; Zhu, B.; Jiang, S.; Chen, X.; Xu, C.-Y. Changes in Forest Net Primary Productivity in the Yangtze River Basin and Its Relationship with Climate Change and Human Activities. *Remote Sens.* **2019**, *11*, 1451. [\[CrossRef\]](#)
21. Jiang, H.; Xu, X.; Guan, M.; Wang, L.; Huang, Y.; Jiang, Y. Determining the contributions of climate change and human activities to vegetation dynamics in agro-pastoral transitional zone of northern China from 2000 to 2015. *Sci. Total Environ.* **2020**, *718*, 134871. [\[CrossRef\]](#)
22. Ugbaje, S.U.; Odeh, I.O.A.; Bishop, T.F.A.; Li, J. Assessing the spatio-temporal variability of vegetation productivity in Africa: Quantifying the relative roles of climate variability and human activities. *Int. J. Digit. Earth* **2017**, *10*, 879–900. [\[CrossRef\]](#)
23. Haberl, H.; Erb, K.H.; Krausmann, F.; Gaube, V.; Bondeau, A.; Plutzer, C.; Gingrich, S.; Lucht, W.; Fischer-Kowalski, M. Quantifying and mapping the human appropriation of net primary production in earth's terrestrial ecosystems. *Proc. Natl. Acad. Sci. USA* **2007**, *104*, 12942–12945. [\[CrossRef\]](#) [\[PubMed\]](#)
24. Xu, D.Y.; Kang, X.W.; Zhuang, D.F.; Pan, J.J. Multi-scale quantitative assessment of the relative roles of climate change and human activities in desertification—A case study of the Ordos Plateau, China. *J. Arid Environ.* **2010**, *74*, 498–507. [\[CrossRef\]](#)
25. Naeem, S.; Zhang, Y.; Tian, J.; Qamer, F.M.; Latif, A.; Paul, P.K. Quantifying the Impacts of Anthropogenic Activities and Climate Variations on Vegetation Productivity Changes in China from 1985 to 2015. *Remote Sens.* **2020**, *12*, 1113. [\[CrossRef\]](#)
26. Ren, G.; Ding, Y.; Zhao, Z.; Zheng, J.; Wu, T.; Tang, G.; Xu, Y. Recent progress in studies of climate change in China. *Adv. Atmos. Sci.* **2012**, *29*, 958–977. [\[CrossRef\]](#)
27. Wang, C.; Jiang, Q.o.; Engel, B.; Mercado, J.A.V.; Zhang, Z. Analysis on net primary productivity change of forests and its multi-level driving mechanism—A case study in Changbai Mountains in Northeast China. *Technol. Forecast. Soc. Chang.* **2020**, *153*, 119939. [\[CrossRef\]](#)
28. Hu, Q.; Pan, X.; Shao, C.; Zhang, D.; Wang, X.; Wei, X. Distribution and Variation of China Agricultural Heat Resources in 1961–2010. *Chin. J. Agrometeorol.* **2014**, *35*, 119–127. (In Chinese)
29. Li, K.; Tong, Z.; Liu, X.; Zhang, J.; Tong, S. Quantitative assessment and driving force analysis of vegetation drought risk to climate change: Methodology and application in Northeast China. *Agric. For. Meteorol.* **2020**, *282*, 107865. [\[CrossRef\]](#)
30. He, B.; Lue, A.; Wu, J.; Zhao, L.; Liu, M. Drought hazard assessment and spatial characteristics analysis in China. *J. Geogr. Sci.* **2011**, *21*, 235–249. [\[CrossRef\]](#)

31. Jiang, S.; Wang, J.; Zhao, Y.; Shang, Y.; Gao, X.; Li, H.; Wang, Q.; Zhu, Y. Sustainability of water resources for agriculture considering grain production, trade and consumption in China from 2004 to 2013. *J. Clean Prod.* **2017**, *149*, 1210–1218. [\[CrossRef\]](#)
32. Mao, D.; Wang, Z.; Wu, J.; Wu, B.; Zeng, Y.; Song, K.; Yi, K.; Luo, L. China's wetlands loss to urban expansion. *Land Degrad. Dev.* **2018**, *29*, 2644–2657. [\[CrossRef\]](#)
33. Mao, D.; He, X.; Wang, Z.; Tian, Y.; Xiang, H.; Yu, H.; Man, W.; Jia, M.; Ren, C.; Zheng, H. Diverse policies leading to contrasting impacts on land cover and ecosystem services in Northeast China. *J. Clean Prod.* **2019**, *240*, 117961. [\[CrossRef\]](#)
34. Mao, D.; Wang, Z.; Luo, L.; Ren, C. Integrating AVHRR and MODIS data to monitor NDVI changes and their relationships with climatic parameters in Northeast China. *Int. J. Appl. Earth Obs. Geoinf.* **2012**, *18*, 528–536. [\[CrossRef\]](#)
35. Geng, R.; Zhao, Y.; Cui, Q.; Qin, F. Representation of modern pollen assemblages with respect to vegetation and climate in Northeast China. *Quat. Int.* **2019**, *532*, 126–137. [\[CrossRef\]](#)
36. Xin, F.; Xiao, X.; Dong, J.; Zhang, G.; Zhang, Y.; Wu, X.; Li, X.; Zou, Z.; Ma, J.; Du, G.; et al. Large increases of paddy rice area, gross primary production, and grain production in Northeast China during 2000–2017. *Sci. Total Environ.* **2020**, *711*, 135183. [\[CrossRef\]](#)
37. Zhou, H.; Yue, X.; Lei, Y.; Zhang, T.; Tian, C.; Ma, Y.; Cao, Y. Responses of gross primary productivity to diffuse radiation at global FLUXNET sites. *Atmos. Environ.* **2021**, *244*, 117905. [\[CrossRef\]](#)
38. Potter, C.S.; Randerson, J.T.; Field, C.B.; Matson, P.A.; Vitousek, P.M.; Mooney, H.A.; Klooster, S.A. Terrestrial Ecosystem Production: A Process Model Based on Global Satellite and Surface Data. *Glob. Biogeochem. Cycle* **1993**, *7*, 811–841. [\[CrossRef\]](#)
39. Zhu, W.Q.; Pan, Y.Z.; He, H.; Yu, D.Y.; Hu, H.B. Simulation of maximum light use efficiency for some typical vegetation types in China. *Chin. Sci. Bull.* **2006**, *51*, 457–463. [\[CrossRef\]](#)
40. Lieth, H. Modeling the primary productivity of the world. *Nat. Resour.* **1972**, *8*, 5–10.
41. Hurst, H. Long Term Storage Capacity of Reservoirs. *Trans. Am. Soc. Civil Eng.* **1951**, *116*, 770–799. [\[CrossRef\]](#)
42. Wang, Y.; Liu, X.; Ren, G.; Yang, G.; Feng, Y. Analysis of the spatiotemporal variability of droughts and the effects of drought on potato production in northern China. *Agric. For. Meteorol.* **2019**, *264*, 334–342. [\[CrossRef\]](#)
43. Wu, D.; Zhao, X.; Liang, S.; Zhou, T.; Huang, K.; Tang, B.; Zhao, W. Time-lag effects of global vegetation responses to climate change. *Glob. Change Biol.* **2015**, *21*, 3520–3531. [\[CrossRef\]](#) [\[PubMed\]](#)
44. Liu, Y.; Yang, Y.; Wang, Q.; Du, X.; Li, J.; Gang, C.; Zhou, W.; Wang, Z. Evaluating the responses of net primary productivity and carbon use efficiency of global grassland to climate variability along an aridity gradient. *Sci. Total Environ.* **2019**, *652*, 671–682. [\[CrossRef\]](#)
45. Dewar, R.C.; Medlyn, B.E.; McMurtrie, R.E. A mechanistic analysis of light and carbon use efficiencies. *Plant Cell Environ.* **1998**, *21*, 573–588. [\[CrossRef\]](#)
46. Gifford, R.M. Plant respiration in productivity models: Conceptualisation, representation and issues for global terrestrial carbon-cycle research. *Funct. Plant Biol.* **2003**, *30*, 171–186. [\[CrossRef\]](#) [\[PubMed\]](#)
47. Waring, R.H.; Landsberg, J.J.; Williams, M. Net primary production of forests: A constant fraction of gross primary production? *Tree Physiol.* **1998**, *18*, 129–134. [\[CrossRef\]](#) [\[PubMed\]](#)
48. Zeng, Y.; Yang, X.; Fang, N.; Shi, Z. Large-scale afforestation significantly increases permanent surface water in China's vegetation restoration regions. *Agric. For. Meteorol.* **2020**, *290*, 108001. [\[CrossRef\]](#)
49. Tao, F.; Zhang, Z. Dynamic responses of terrestrial ecosystems structure and function to climate change in China. *J. Geophys. Res.* **2010**, *115*, G03003. [\[CrossRef\]](#)
50. Tian, Z.; Xu, H.; Sun, L.; Fan, D.; Fischer, G.; Zhong, H.; Zhang, P.; Pope, E.; Kent, C.; Wu, W. Using a cross-scale simulation tool to assess future maize production under multiple climate change scenarios: An application to the Northeast Farming Region of China. *Clim. Serv.* **2020**, *18*, 100150. [\[CrossRef\]](#)
51. Sun, G.; Mu, M. Assessing the characteristics of net primary production due to future climate change and CO₂ under RCP4.5 in China. *Ecol. Complex.* **2018**, *34*, 58–68. [\[CrossRef\]](#)
52. Jiapaer, G.; Liang, S.; Yi, Q.; Liu, J. Vegetation dynamics and responses to recent climate change in Xinjiang using leaf area index as an indicator. *Ecol. Indic.* **2015**, *58*, 64–76.
53. Wang, J.; Rich, P.M.; Price, K.P. Temporal responses of NDVI to precipitation and temperature in the central Great Plains, USA. *Int. J. Remote Sens.* **2003**, *24*, 2345–2364. [\[CrossRef\]](#)
54. Horion, S.; Cornet, Y.; Erpicum, M.; Tychon, B. Studying interactions between climate variability and vegetation dynamic using a phenology based approach. *Int. J. Appl. Earth Obs. Geoinf.* **2013**, *20*, 20–32. [\[CrossRef\]](#)
55. Lu, N.; Wilske, B.; Ni, J.; John, R.; Chen, J. Climate change in Inner Mongolia from 1955 to 2005—trends at regional, biome and local scales. *Environ. Res. Lett.* **2009**, *4*, 045006. [\[CrossRef\]](#)
56. Mowll, W.; Blumenthal, D.M.; Cherwin, K.; Smith, A.; Symstad, A.J.; Vermeire, L.T.; Collins, S.L.; Smith, M.D.; Knapp, A.K. Climatic controls of aboveground net primary production in semi-arid grasslands along a latitudinal gradient portend low sensitivity to warming. *Oecologia* **2015**, *177*, 959–969. [\[CrossRef\]](#) [\[PubMed\]](#)
57. Zeng, B.; Yang, T. Impacts of climate warming on vegetation in Qaidam Area from 1990 to 2003. *Environ. Monit. Assess.* **2008**, *144*, 403–417. [\[CrossRef\]](#) [\[PubMed\]](#)
58. Chen, Y.; Mu, S.; Sun, Z.; Gang, C.; Li, J.; Padarian, J.; Groisman, P.; Chen, J.; Li, S. Grassland Carbon Sequestration Ability in China: A New Perspective from Terrestrial Aridity Zones. *Rangel. Ecol. Manag.* **2016**, *69*, 84–94. [\[CrossRef\]](#)

59. Song, Y.; Ma, M. Variation of AVHRR NDVI and its Relationship with Climate in Chinese Arid and Cold Regions. *J. Remote Sens.* **2008**, *12*, 499–505. (In Chinese)
60. Zhang, Y.; Peng, C.; Li, W.; Tian, L.; Zhu, Q.; Chen, H.; Fang, X.; Zhang, G.; Liu, G.; Mu, X.; et al. Multiple afforestation programs accelerate the greenness in the ‘Three North’ region of China from 1982 to 2013. *Ecol. Indic.* **2016**, *61*, 404–412. [[CrossRef](#)]
61. Fu, B.J.; Liu, S.L.; Ma, K.M.; Zhu, Y.G. Relationships between soil characteristics, topography and plant diversity in a heterogeneous deciduous broad-leaved forest near Beijing, China. *Plant Soil* **2004**, *261*, 47–54. [[CrossRef](#)]
62. Cheng, Y.; Li, P.; Xu, G.; Li, Z.; Gao, H.; Zhao, B.; Wang, T.; Wang, F.; Cheng, S. Effects of soil erosion and land use on spatial distribution of soil total phosphorus in a small watershed on the Loess Plateau, China. *Soil Tillage Res.* **2018**, *184*, 142–152. [[CrossRef](#)]
63. Liu, Z.; Yang, J.; Chang, Y.; Weisberg, P.J.; He, H.S. Spatial patterns and drivers of fire occurrence and its future trend under climate change in a boreal forest of Northeast China. *Glob. Change Biol.* **2012**, *18*, 2041–2056. [[CrossRef](#)]
64. Yang, G.; Shu, L.F.; Di, X.Y. Prediction on the changes of forest fire danger rating in Great Xing’an Mountain region of Northeast China in the 21st century under effects of climate change. *Chin. J. Appl. Ecol.* **2012**, *23*, 3236–3242. (In Chinese)
65. Prăvălie, R.; Patriche, C.; Țișcovschi, A.; Dumitrașcu, M.; Săvulescu, I.; Sîrodoev, I.; Bandoc, G. Recent spatio-temporal changes of land sensitivity to degradation in Romania due to climate change and human activities: An approach based on multiple environmental quality indicators. *Ecol. Indic.* **2020**, *118*, 106755. [[CrossRef](#)]
66. Liu, X.; Dong, G.; Xue, Z.; Lu, X.; Jiang, M.; Zhang, Y. Carbon sequestration potential change after marshlands conversion to croplands in the Northeast China between 1982 and 2010. *Ecol. Eng.* **2014**, *70*, 402–405. [[CrossRef](#)]
67. Tian, J.; Wang, B.; Zhang, C.; Li, W.; Wang, S. Mechanism of regional land use transition in underdeveloped areas of China: A case study of northeast China. *Land Use Policy* **2020**, *94*, 104538. [[CrossRef](#)]
68. Liu, X.; Dong, G.; Wang, X.; Xue, Z.; Jiang, M.; Lu, X.; Zhang, Y. Characterizing the spatial pattern of marshlands in the Sanjiang Plain, Northeast China. *Ecol. Eng.* **2013**, *53*, 335–342. [[CrossRef](#)]
69. Chen, H.; Zhang, W.; Gao, H.; Nie, N. Climate Change and Anthropogenic Impacts on Wetland and Agriculture in the Songnen and Sanjiang Plain, Northeast China. *Remote Sens.* **2018**, *10*, 356. [[CrossRef](#)]
70. Wang, L.L.; Song, C.C.; Ge, R.J.; Song, Y.Y.; Liu, D.Y. Soil organic carbon storage under different land-use types in Sanjiang Plain. *China Environ. Sci.* **2009**, *29*, 656–660. (In Chinese)
71. Piao, S.; Fang, J.; He, J. Variations in Vegetation Net Primary Production in the Qinghai-Xizang Plateau, China, from 1982 to 1999. *Clim. Change* **2006**, *74*, 253–267. [[CrossRef](#)]